Title
Differential Gene Expression in the Periodontal Tissues of 6-week-old Mouse Incisors Undergoing Accelerated Renewal

Author
Miresmaili, Armin

Publication Date
2021

Peer reviewed|Thesis/dissertation

Differential Gene Expression in the Periodontal Tissues of 6-week-old Mouse Incisors

by
Armin Miresmaili

THESIS
Submitted in partial satisfaction of the requirements for degree of
MASTER OF SCIENCE

in

Oral and Craniofacial Sciences

in the

GRADUATE DIVISION
of the
UNIVERSITY OF CALIFORNIA, SAN FRANCISCO

Approved:

DocuSigned by:
Andrew H. Jheon
F365EA7416024CA...

Andrew H. Jheon
Chair

DocuSigned by:
Alice Goodwin
[illegible]EF...

Alice Goodwin

DocuSigned by:
Christine Hong
CE6EAA6FBA31451...

Christine Hong

Committee Members

Differential Gene Expression in the Periodontal Tissues of 6-week-old Mouse Incisors Undergoing Accelerated Renewal

Armin S. Miresmaili

Abstract

Objectives: The Order Rodentia is characterized, in part, by their continuously erupting or renewing incisors. Since little is known about the attachment of the incisors to alveolar bone, we aim to identify differentially expressed genes in the periodontal ligament (PDL)-like tissue of the mouse incisor during normal and accelerated renewal. We confirmed that mouse incisors grow faster when out of occlusion. We hypothesize that this accelerated renewal is associated with changes in gene expression within the PDL-like tissue on the lingual surface of the mouse incisor that allows for increased turnover of tooth-bone attachment. Global profiling of gene expression during periods of accelerated incisor renewal will identify genes and genetic networks that will advance understanding of PDL turnover, and ultimately, may allow us to accelerate orthodontic tooth movement (OTM) in mouse molars and human teeth.

Methods: Sample groups consisted of 6-week-old control (n=3) and experimental (n=3) FVB/NJ mice. Experimental mice had one incisor cut at the tip (2-3mm), and incisor renewal was allowed for 24 hours. Control mice were unaltered. Mice were euthanized, mandibular incisors were extracted, soft tissues attached to the extracted incisors were collected, and total RNA was isolated to perform global profiling of gene expression using bulk RNAseq analysis. The total number of samples (n=9) include control (n=3), the non-cut incisor from experimental mice (n=3), and the cut incisor from experimental mice (n=3). From a list of differentially expressed

genes, three specific genes were selected for further evaluation using quantative *in situ* hybridization (RNAscope).

Results: Bulk RNAseq revealed a significant increase ($p<.01$) in the expression of 365 genes in cut incisors and non-cut contralateral incisors relative to control (CTRL). *Lgals7*, *Ovol1*, and *Stx19* were selected for potential promising roles during accelerated incisor renewal. RNAscope analysis confirmed the upregulation of these genes in soft tissue associated with the cut experimental incisor but expression was specific to gingival tissue.

Conclusion: We identified three up-regulated genes, *Lgals7*, *Ovol1*, and *Stx19*, that were associated with the mouse incisor undergoing accelerated renewal. These genes may play key roles in gingival remodeling during tooth movement, such as tooth eruption, drift, and OTM. Further experiments will be performed to determine the roles of these candidate genes in gingival homeostasis during OTM, and to isolate differentially expressed genes specifically expressed in PDL-like tissue. We envision that the accelerated mouse incisor model will be valuable in advancing cellular and molecular understanding of soft tissue turnover (PDL and gingiva) during OTM.

Table of Contents

List of Figures

List of Tables

1. Introduction

1.1 Orthodontics and orthodontic tooth movement

Some of the first evidence of orthodontics in practice were recorded from the times of the ancient Egyptians and Greeks tens of thousands of years ago (Weinberger 1934). Initial attempts at orthodontic tooth movement (OTM) were performed with crude materials, no attention to sterility, and the use of archaic placement methods. The practice of orthodontics as we know it today came about in the last 120 years. Practical appliances started being utilized and refined in the 1900s, and what we use today are for the most part refinements on these appliances (Wahl 2005).

Malocclusion, previously termed "irregularities," were "regulated" originally for cosmetic purposes. Then over time as empiricism gave way to objectivity and the scientific method, greater focus was placed on occlusion and stability (Wahl 2005). In recent decades, orthodontic techniques have become increasingly refined to catch up with the increasing prevalence of malocclusion. Odds are that you have had braces yourself or know a few people who have. So many are treated for malocclusion that it has become a childhood rite of passage. This high prevalence is synonymous with an epidemic but has become so normalized in our society that it is not regularly thought of as such. Available evidence points to the epidemic arising due to behavioral and environmental changes with the advent of agriculture, sedentism, and industrialization (Kahn et al. 2020). Softening diets and processed foods, that our ancestors never had, have contributed to underdeveloped jaws, a key factor in malocclusion (Kahn et al. 2020).

Malocclusions can be skeletal and/or dental in origin. Skeletal issues arise when the maxilla and/or mandible are under- or over- developed, leading to discrepancies in how the skeletal components relate to one another. If the jaws are not aligned properly, the dentition residing within cannot come together to form a proper bite (Joshi et al. 2014). However, dental issues can still persist when the skeletal components are in ideal relation, such as in the form of open bites, crossbites, crowding, spacing, and impactions. Understanding the specifics of malocclusion is now more important than ever. While skeletal discrepancies most often need surgical intervention, dental issues can be corrected with OTM.

Teeth can be moved to ideal positions utilizing OTM, a process during which external forces are applied to the teeth causing changes in the surrounding bone mediated by the periodontal ligament (PDL) (Jiang et al. 2016). The changes in the PDL allows teeth to translate through the bone - a process where bone is relieved on one side of the tooth and built up on the other as it slowly incrementally moves in the direction of force application (Holland et al. 2019). However, OTM is only possible through the existence of the PDL as it guides bone turnover, and without it tooth movement would not be possible (Feller et al. 2015). The necessity of the PDL in OTM is why we will be investigating gene expression in the PDL-like tissue associated with mouse incisor.

1.2 Periodontal Ligament (PDL)

The PDL is well studied in periodontology, but despite being essential in our ability to move teeth in the orthodontic field, little is known about the molecular mechanisms involved in the PDL during tooth movement. The PDL is essential in anchoring teeth to the alveolar bony housing and in any tooth movement such as tooth eruption, drift, and OTM. The absolute

necessity of the PDL in tooth movement is demonstrated by the fact that ankylosed teeth (teeth without PDL) and dental implants cannot undergo any movement (Feller et al. 2015).

During orthodontic treatment, controlled forces are applied to the teeth. The forces cause compression and tension strains within the PDL-tooth complex leading to remodeling of the alveolar housing (Jiang et al. 2016). The rate of remodeling varies based on duration, magnitude of the force, and potential yet unknown genetic components. At the molecular level, how exactly these external forces result in OTM is unclear. While a few genes have been identified to be involved in this process, global gene expression profiling of PDL tissue during accelerated renewal using powerful transcriptome sequencing techniques has yet to be completed.

1.3 Mouse as an experimental model

Mus musculus, the house mouse, makes an excellent choice for our experimental model. Mice have a fully sequenced genome with 99% similarity to humans (Vandamme 2014). Biologically, they are very similar to humans in multiple tissues and organs. Genetic alterations in mice can mimic almost any human disease or condition. The mouse genome was published in 2002 and is approximately 3,500 million base pairs in length and contains over 22,000 protein-coding genes (Ensemble 2020). Mice are also cost effective, easy to maintain, relatively inexpensive, and can be bred in a short timeline to increase study populations. Their small size also helps facilitate large scale studies (Vandamme 2014).

Mouse models have been used extensively in orthodontic research. Mice are valuable to demonstrate changes in the alveolar bone and teeth during OTM and generate tractable results that may be ultimately applied to patients in the clinic. With careful application, orthodontic appliances can be placed on mouse dentition, and effects of OTM on teeth, PDL, and alveolar

bone can be studied at the tissue, cellular, and molecular level to advance mechanistic understanding of OTM.

An excellent genetic/molecular toolbox has been developed to facilitate our study. Given that the genome has been sequenced, alterations in gene transcription can be analyzed at nearly any time in most every tissue in the mouse. Mice can also be readily manipulated genetically, allowing us to create transgenic (e.g., knockout) animals that can model human phenotypes. Such mouse models offer beneficial tools for future exploration into specific genes and genetic networks and mechanistic understanding of OTM (Babb et al. 2019).

1.4 Mouse Incisor

Mice possess a reduced dentition with three molars and one incisor in each quadrant. Mouse molar crowns are composed of dentin covered in enamel and are "rooted" like human teeth. In mouse incisors, enamel is only present on the labial surface and not on the lingual surface. We know the lingual surface (dentin and/or cementum) must be attached to alveolar bone via PDL-like tissue. Comprehensive characterization of this dentin/cementum, PDL-like tissue interface has yet to be performed. On the labial side, it is unclear how the enamel of the unerupted portion of the incisor is attached to the alveolar bone, if at all. The enamel of the unerupted incisor remains bound to ameloblasts, which is bound to the stratum intermedium, a derivative of the dental follicle. Upon eruption, the ameloblasts are sloughed off and enamel is exposed to the oral cavity. Similarly, human enamel is surrounded by ameloblasts and the dental follicle when unerupted but exposed to the oral cavity once erupted. Throughout the lifetime of the mouse, the incisors erupt or renew continuously, which along with the process of "gnawing" maintain their constant length and keep them sharp, ready for defense and predation. A great portion of the

incisor is unerupted and located within the maxilla and mandible, with only the distal ends erupting through the gingiva in the oral cavity. The main components of this interface are the tooth itself, the regions of attachment to the mouse skull, and the region of proliferation at the proximal base. A primary goal of my study is to understand how the continuously renewing mouse incisor interacts with the surrounding periodontal complex such as the alveolar bone and soft tissues including gingival and PDL-like tissues (Balic 2019).

Continuously renewing incisors are a defining feature of all rodents (Balic 2019). While humans cannot regrow their adult teeth, this renewal occurs in mice as they wear down their four front incisors, leading to a completely new tooth in approximately 35-45 days (Sharir et al. 2019). That is approximately 2-3 mm a week of incisor renewal. This growth in mice can also vary with age and season (Klevezal, 2010). If incisors are damaged, for example when the distal tip is cut out of occlusion, this rate of renewal may increase (Dolores, 2016). Mice incisors may also grow past their normal length when developing out of occlusion, a phenomenon that occurs when jaws or teeth are misaligned preventing normal contact and attrition (Dolores, 2016).

Physical stimuli such as unopposed occlusion and trauma are followed by a cellular response leading to the propagation of the incisor. As the tip of the incisor gets ground down, a pool of epithelial and mesenchymal stem cells (ESCs and MSCs, respectively) at the proximal incisor end deep inside the jaw, constantly renew the incisor and push the incisor forward to erupt out of gingival tissue (Balic 2019). The mouse incisor is the site of five cell populations proliferating in harmony: ameloblasts, odontoblasts, pulp cells, endothelial cells, and the PDL cells. Cells displaced from the proximal end of the tooth, toward the periphery, mature to perform their specific functions.

1.5 Bulk RNA-sequencing (RNAseq)

RNA molecules are essential elements of all living cells (Hrdlickova et al. 2017). They are what turn the genomic language into functional RNAs and proteins, thus regulating the organism in its entirety. The transcriptome is the complete set of RNA transcripts (mRNAs) in a cell. This data of course changes as we can only analyze transcripts that are expressed at a specific space and time. Understanding the transcriptome is crucial for learning about the functional components of the genome and revealing what molecular units of cells and tissues are responsible for their current status (Wang et al. 2009).

Bulk RNAseq will be utilized to complete global gene expression profiling of PDL tissue during accelerated mouse incisor renewal. RNAseq provides an insight into the transcriptome of the cell using high-throughput methods. Initial gene expression studies relied on low-throughput methods, such as northern blots and quantitative polymerase chain reaction (qPCR), that are limited to measuring transcripts of known candidate genes. Beyond simply quantifying gene expression, RNAseq is a non-biased approach that can help facilitate the discovery of novel transcripts, identification of alternatively spliced genes, and detection of allele-specific expression (Kukurba and Montgomery 2015). Being able to isolate expressed genes (gene transcripts/mRNA) and their quantities during accelerated renewal will give us insight into what governs tooth movement. However, reading the transcriptome is a monumental task on its own as it may contain tens of thousands of genes.

1.6 Significance

Our understanding of the PDL-like tissue associated with mouse incisors is limited because there are few prior studies. While a few suspected genes are known to be involved in OTM, global gene expression profiling of PDL-like tissue during accelerated incisor renewal using RNAseq has yet to be performed. In this study, we aim to identify differentially expressed genes in the PDL-like tissue of the mouse incisor during normal and accelerated renewal. The broader goal of this study is to determine whether the differentially expressed genes in PDL-like tissue are also important in the PDL during OTM, which may ultimately be applied to human OTM.

In this project, we aim to identify differentially expressed genes in PDL-like tissue of the mouse incisor during normal and accelerated renewal.

- We confirmed that mouse incisors grow faster when out of occlusion, and this phenomenon may be associated with changes in gene expression within the PDL-like tissue attached to the lingual incisor surface.
- Global profiling of gene expression during increased incisor renewal will allow us to identify important genes involved with soft tissue turnover/homeostasis.
- These identified differentially expressed genes may be important for accelerated OTM in mouse molars and human teeth.

We reason that a better understanding of the incisor attachment to the mouse mandible and what factors allow for faster gingival and PDL-like tissue turnover during increased incisor renewal will identify potential mechanisms (genes and signaling pathways) to accelerate OTM in humans.

2. Materials and Methods

2.1 Design

Control vs Incisor-Cut Mice

Sample groups consisted of 6-week-old control (n=3), non-cut experimental (n=-3), and cut experimental (n=3) FVB/NJ mice (Jackson laboratory). Experimental mice had one incisor cut at the tip (2-3mm), and incisor renewal was allowed for 24 hours. Control mice were unaltered. Mice were euthanized, mandibular incisors were extracted, soft tissues attached to the extracted incisors were collected (presumably PDL cells), and RNA was isolated for bulk RNAseq analysis. Total RNA was isolated using the RNeasy Plus Mini kit (Qiagen, Valencia, CA, USA) following manufacturer's directions. This provided two samples from each experimental mouse, once cut incisor and one uncut, as well as one uncut incisor from the control mouse. The total RNA isolated was utilized for RNAseq analysis. Figure 1 shows overall project flow.

2.2 Global Identification of Genes using bulk RNAseq

Bulk RNAseq experiments were performed by the UCSF SABRE Functional Genomics Core (https://functionalgenomicscore.ucsf.edu/). Briefly, total RNA quality was assessed by spectrophotometry (NanoDrop; Thermo Fisher Scientific Inc., Rockford, IL, USA) and Agilent 2100 Bioanalyzer (Agilent Technologies, Santa Clara, CA, USA). RNA sequencing libraries were generated using the TruSeq stranded mRNA sample prep kits with multiplexing primers, according to the manufacturer's protocol (Illumina, San Diego, CA, USA), and library concentrations were measured using KAPA Library Quantification Kits (Kapa Biosystems, Inc.). Equal amounts of indexed libraries were pooled and sequenced on the Illumina HiSeq 2500 (Illumina). Data analysis involved demultiplexing the results, trimming adapter sequences from

the reads, and aligning unique reads to the mouse genome (mm10). Sequence alignment and splice junction estimation were performed using software programs Bowtie2 (http://bowtie-bio.sourceforge.net/bowtie2/index.shtml; Langmead and Salzberg, 2012) and TopHat (http://tophat.cbcb.umd.edu/; Trapnell et al., 2009), respectively. For differential expression testing, the genomic alignments were restricted to those mapping to an annotated transcriptome provided by Ensembl (Flicek et al., 2014). This subset of mappings was aggregated on a per-gene basis as raw input for the program DESeq (Anders and Huber, 2010).

Gene ontology (GO) analysis was performed using GO Consortium (Ashburner et al. 2000). The Gene Ontology resource provides a computational representation of our current scientific knowledge about the functions of genes (or, more properly, the protein and non-coding RNA molecules produced by genes). Enriched GO terms for biological processes, molecular function and cellular components were detected and clustered using the gene IDs for which False Discovery Rate (FDR) was < 0.05 and default parameters for Functional Annotation Clustering.

Further identification of candidate genes was completed through background research using the Alliance of Genome Resources and Mouse Genome Informatics (Kishore et al. 2020) automated gene summary generation. Additional supporting data was collected from the Human Gene Database (Stelzer et al. 2016), the knowledgebase automatically integrates gene-centric data including genomic, transcriptomic, proteomic, genetic, clinical and functional information from over 170 genetic databases. After extensive literature search of the candidate genes (total of 365 genes) presenting with a p-value < 0.01 and (FDR) < 0.05, three candidate genes were selected for RNAscope confirmation: *Lgals7*, *Ovol1*, and *Stx19*. These genes were selected based on their potential involvement in accelerated renewal of the incisors as well as the greatest delta in expression; genes selected participated in growth signaling, growth control, or bone remodeling.

2.3 Verification of genes using RNAScope

RNAscope 2.5 HD Red detection kit (Advanced Cell Diagnostics, ACD; Cat No. 322350) was used following the manufacturer's instructions. Six-week old mice with cut mandibular incisors or control were euthanized and their oral mucosa/tongue tissues removed and placed into a 10% neutral buffered formalin solution at room temperature for ~20 hours. Tissues were then washed in phosphate buffered saline (PBS), paraffin processed, and embedded in paraffin blocks. Paraffin blocks were sectioned at 7µm sections on a microtome. ACD - Mm-*Lgals7* (Cat No. 4935921); Mm-*Ovol1* (Cat No. 845271); Mm-*Stx19-01* (Cat No. 886091). *DapB* (negative control target probe (Cat No. 310043) was also used and consistently showed little to no background staining.

2.4 Image Acquisition

Fluorescent and bright-field images were taken using a DM5000B microscope with a DFC500 camera (Leica, Wetzlar, Germany). For confocal images, a Leica-TCS SP5 microscope was used.

2.5 Image Analysis Software

Fiji ImageJ was used to analyze the RNAscope data. Technical notes were provided by the probe manufacturer (ACD). Field of view was capped at two gigapixels to count cells and punctate dots within cell boundaries due to ImageJ's limited capability in handling large, high-resolution images. To identify the punctate staining representing activated RNA molecules, the color deconvolution tool was used to isolate the distinct nuclear marker stain. One dot of staining represents one RNA transcript in intact cells. Multiplex fluorescent image analysis and particle analysis functions were then used to count the positive punctate staining **(Figure 2.)**. Manual count confirmation was completed on several samples to verify the analysis software results and reproducibility.

3. Results

3.1 Identification of differentially expressed genes in mandibular incisors undergoing accelerated renewal using bulk RNAseq analysis

RNAseq from the UCSF SABRE Functional Genomics Core returned a data set of 43,433 genes for each of our 6 samples. As one can imagine, it can be a tedious process to sift through 43K columns of data to find what could be a potential gene of interest for future study. We began data sorting by removing simple metabolic genes/background genes. Then null values were removed or genes that did not return any values, which may be due to the low or no expression of the genes in the sample. We then applied a significance value of $p < 0.01$ to the delta comparison of the mean RNA counts of the experimental incisor compared to the control mouse incisor. This strict p-value value was used to demonstrate substantial evidence of change, while giving us a confidence level of >99%. Application of this parameter reduced our list of differentially expressed genes significantly to 365 (Figure 3). From here we reduced our list of differentially expressed genes by only considering genes with a false discovery rate of less than 0.05 (FDR < 0.05). The same metrics were applied to genes from the cut experimental incisor vs control to the uncut incisor from the experimental mouse vs control which yielded 89 and 96 genes, respectively, from the two comparison groups, which can be visualized in Figures 3-5. Gene ontology and background research was completed on this group of genes, an example of this can be seen in Table 1. This data elucidated the potential of these genes to be involved in the accelerated renewal process. The expression levels of these genes can be visualized in RNA heat maps (Figure 6-7). This group was further narrowed by evaluating for the largest deltas in combination with having the largest bodies of supporting functions most likely to be related to the biological processes known to be involved in tooth movement. The application of these

parameters yielded 3 candidate genes for further analysis using RNAscope to check expression level and pattern in the tissues of the dentoalveolar junction/PDL-like tissue.

3.2 Selection of genes of interest for further study

The three genes selected for potential promising roles in accelerated renewal were *Lgals7*, *Ovol1*, and *Stx19*. As demonstrated in Figure 3, a marked increase in expression was observed in cut experimental incisors relative to control (CTRL) and uncut experimental incisor (Figure 8). Further background research was conducted on these genes and compiled demonstrating their potential involvement in accelerated incisor renewal.

Lgals7 - Lectin, Galactoside-Binding, Soluble, 7

Galectins, discovered in 1994, are a family of soluble lectins with primary structural homology in their carbohydrate-recognition domains (CRDs) (Barondes et al. 1994). Glycan-binding proteins are specifically expressed epithelial cells, including keratinocytes and mainly in stratified squamous epithelium. They are commonly overexpressed in cancer cells and cancer-associated stromal cells. Galectins are involved in the pathogenesis of inflammatory skin diseases by affecting the functions of immune cells and correlated with the aggressiveness of the tumor and the metastatic phenotype because of their ability to induce local immunosuppression and to confer cancer cells with resistance to apoptosis.

Galectin-7, a regulator of apoptosis, also known as GAL7 or LGALS7, is the subgroup of dimeric galectins with two identical CRD subunits. Galectin-7 was found in the stratified squamous epithelium in the gut and skin, including the mucosal epithelium of digestive tracts of mice (Nio-Kobayashi 2017). Gal-7 re-expression affects the regulation of molecular networks in

diverse cancer hallmarks, such as metabolism, growth control, invasion, and evasion of apoptosis. Gal-7 is an adverse prognosticator for ovarian cancer, non-metastatic clear cell renal cell carcinoma, breast cancer, and head and neck squamous cell carcinoma (Schulz et al. 2017; Wang et al. 2016; Trebo et al. 2020; Chen et al. 2018). Galectin-7 played a critical role in promoting tumorigenesis and metastatic progression by enhancing the transcriptional activity of TCF3 transcription factor through elevating MMP-9 expression. Gal-7 knockdown attenuates TGF-beta1-induced apoptosis in bronchial epithelial cells through inactivation of the JNK pathway (Sun and Zhang 2019). It acts as antifibrotic factors in liver fibrosis (Inagaki et al.2008). Measurement of scGal-7 content in tape-stripped samples was useful for the evaluation of the skin barrier function in dry skin conditions such as atopic dermatitis (Niiyama et al. 2016).

Ovol1 - OVO homologue-like 1

OVO homologue-like 1 (Ovol1) is a transcription factor that regulates proliferation and differentiation of progenitor cells in multiple tissues such as epithelial tissues of hair follicles, skin, kidney, in rodent pancreas, as well as germinal epithelium (Vetere et al. 2010; Li et al. 2005; Tsuji et al. 2018). Loss of *Ovol1* enhances skin inflammation in animal models of atopic dermatitis and psoriasis. Ovol1 is known as one of the epithelial to mesenchymal (EMT)-inducing transcription factors, inhibiting and/or promoting EMT and alteration epithelial cell fate (Kagawa et al. 2019). This function plays an important role during cancer cell metastasis by suppressing zinc finger E-box binding homeobox 1 (Xu et al. 2019). OVOL1 may balance the proliferation and differentiation of pancreatic cells through the downstream target NGN3 (Vetere et al. 2010). Ovol1 can also restrict its own expression by counteracting c-Myb activation and histone acetylation of the Ovol1 promoter (Nair et al. 2007). OVOL1 is required for osteoblast differentiation by inducing BMP2 expression in MC3T3-E1 cells (Min et al. 2019).

Stx19 - Syntaxin 19

Fusion and the specificity of fusion of transport vesicles to target membranes are mediated by soluble N-ethylmaleimide-sensitive factor (NSF) attachment protein (SNAP) receptors (SNAREs). Syntaxin 19 (STX19) is an unusual Qa-SNARE without a C-terminal transmembrane domain. Wild-type STX19 (STX191-294) was localized to the plasma membrane and Rab8-positive tubules, whereas the mutant construct lacking the cysteine-rich domain (STX191-277) was found in the cytoplasm (Ampah et al. 2018). STX19 is predominantly detected in mucosal epithelium of the gut and the skin and interacts specifically with the epidermal growth factor (EGF) receptor (Wang et al. 2016).

3.3 Expression analysis using RNAscope

RNAscope was completed on *Lgals7*, *Ovol1*, and *Stx19* to visualize expression levels and location. The region of interest is from the PDL-like tissue attached to the lingual surface of the mouse incisor, one of the regions where cells were gathered from the extracted incisors for RNAseq (Figure 9).

Regions of interest stained at 20x and 40x magnification (Figures 11-16). A 50-micrometer red line in the top left corner demonstrates overall scale. Control (CTRL) incisors are in the first column, 24HR CTRL (uncut experimental incisor) in the second, and 24 Hr cut experimental incisors in the final column. A generalized marked increase in staining can be seen from left to right over all three genes of interest, demonstrating increased expression (Figures 11-16).

3.4 Confirmation of accelerated incisor renewal when mice incisors are out of occlusion.

We confirmed that the mouse incisors do indeed grow faster when out of occlusion (Figure 16). Measurements were made on 6 mice and 12 incisors total, half of which were cut and allowed to grow for two days. An average of 1.37 mm of growth was measured for the cut experimental incisors and 0.72 mm for the non-cut experimental incisors after the 48-hour period. Thus, the mandibular incisors of FVB/NJ mice on average renew/erupt 0.68 mm per day when cut, and 0.36 mm per day when uncut.

4. Discussion

Accelerated mouse incisor renewal is an intriguing process that is not fully understood. We are aware that damage to the incisor can trigger the process, but the exact mechanisms of this process have not been defined. We hypothesized that this damage to the incisors is associated with changes in the gene expression of PDL-like tissue attached to the lingual surface, and that these genes may be important in tooth movement. With this idea in mind, we set out to identify the genes that are differentially expressed in PDL-like tissue of the mouse incisors during normal and accelerated renewal. We reason that better understanding of the genes and genetic networks in PDL-like tissue that are associated with accelerated incisor renewal will identify potential therapeutic targets to accelerate OTM in humans.

To accomplish our goals we isolated total RNA from soft tissues attached to the extracted mouse incisors during accelerated and normal renewal. RNA was isolated immediately after extraction by scraping off the cells attached to the exfoliated incisors, which included PDL-like cells. Bulk RNAseq was completed on the isolated RNA to profile differentially expressed genes in accelerated vs normal renewal. Candidate genes were selected using statistical significance and background research. *Lgals7*, *Ovol1*, and *Stx19* were selected for further research and RNAscope analysis confirmed the upregulation of these genes and determined their expression pattern.

While clear upregulation was observed in the RNAseq data, as well as the RNAscope images, our goal was to identify differentially expressed genes in the PDL-like tissue. Examining our samples closer, it was clear that the 3 selected genes were mainly expressed in gingiva and not in the PDL-like tissue. This was likely due to our harvesting method, as we isolated more gingival tissue rather than PDL-like tissue. While we sectioned the entire hemi-mandible, getting

distinguishable tissue sections proved to be rather difficult. Alternative methods will be utilized in the future to increase precision of specific tissue site isolation, such as laser microdissection or a more careful collection of soft tissue associated with the lingual incisal surface. Although more technique sensitive, these techniques may provide a more direct view into the PDL-like tissue of the mouse incisor.

Overall, *Lgals7*, *Ovol1*, and *Stx19* demonstrated increased expression in gingival tissues in control and experimental samples. This finding could be due to gingival fiber remodeling during OTM as circular, inter-gingival, trans-septal, dento-gingival, and interpapillary fibers are present in these regions. As the tooth moves through the periosteum, these gingival attachments cannot stay in the same position since it would interfere with dental eruption. These genes may be playing an active role in regulating the gingival tissue, and allowing new fibrous connections to be made, which in itself may be a component signaling pathway for eruption and or periodontal turnover.

Our findings also give us insight into the gingiva during OTM and could be the genetic basis for discovering to what extent the gingiva facilitates or inhibits tooth movement. Ultimately, it will be important to discover all the genes involved in this process. Some next steps will be to overexpress or knockout/delete these genes and study what happens to the rate of incisor renewal. We also mentioned earlier that the non-cut experimental incisor next to the experimental cut incisor also showed accelerated renewal to some degree. Investigating further we saw slight increase in overall gene expression, there was a commonality of 45% of the upregulated genes as well. The reasons why the uncut incisor may be affected is because of physical proximity to the activated cellular proliferation region of cut incisor, or due to changes in mechanical forces since when one incisor is cut, all the gnawing forces will be directed to the

single uncut incisor instead of two. Also, physical pressure/wear on the tooth could be signaling for that incisor to increase its renewal via yet unknown mechanisms.

Clinical implications are also an important takeaway from this study. *Lgals7*, *Ovol1*, and *Stx19* may all be involved to some degree with tissue proliferation based on our RNAscope results so they may be candidate genes for gingival therapy. Patients commonly present with gingival hyperplasia during orthodontic treatment, most often due to hygiene, but sometimes may not be associated with poor hygiene. It would be of interest to ultimately find an inhibitor or agonist for such gingival hyperplasia. There may also be potential for an injectable therapeutic target to restrict or increase gingival turnover depending on what is required. Gingival remodeling is a slow process and it can take some fibers months to properly realign and make new cementum attachments, these therapeutics could speed that process up and prevent de-rotations from gingival strain, for example.

Moving forward, we may collect additional RNA from soft tissues attached to extracted mouse incisors using laser microdissection or regional dissection to focus on the lingual surface. Alternative RNAseq methods such as single cell (sc)RNAseq can be used to cluster gene expression patterns and determine the specific cell types within the PDL-like tissue. scRNAseq would allow us to understand at the single cell level what genes are expressed, in what quantities, and how they differ across cells within a sample, whereas bulk RNAseq does not differentiate among cell types within the sample. Furthermore, we will continue studies on *Lgals7*, *Ovol1*, and *Stx19* and determine their roles in gingival homeostasis during OTM. For example, we will initiate OTM on mouse molars and perform RNAscope to determine whether *Lgals7*, *Ovol1*, and *Stx19* expression is up-regulated in gingiva associated with OTM.

5. Conclusion

In summary, we identified three genes, *Lgals7*, *Ovol1*, and *Stx19* in the soft tissue attached to the mouse incisor that were up-regulated during accelerated renewal. These genes may play key roles in gingival remodeling during tooth movement, such as tooth eruption, drift, and OTM. Further experiments will be performed to determine the roles of these candidate genes during OTM. For example, we will induce OTM in mouse molars and determine whether these genes are up-regulated in gingival tissue associated with molar movement. Furthermore, we will vary the method in which we collected soft tissue to isolate PDL-like tissue attached to the mouse incisor. We feel that the mouse incisor undergoing accelerated renewal is a valuable model to advance cellular and molecular understanding of soft tissues and PDL turnover during OTM.

6. References

1. Stelzer G, Rosen N, Plaschkes I, Zimmerman S, Twik M, Fishilevich S, et al. The genecards suite: from gene data mining to disease genome sequence analyses. Curr Protoc Bioinformatics. 2016 Jun 20;54:1.30.1-1.30.33.

2. Kishore R, Arnaboldi V, Van Slyke CE, Chan J, Nash RS, Urbano JM, et al. Automated generation of gene summaries at the Alliance of Genome Resources. Database (Oxford). 2020 Jan 1;2020.

3. Gene Ontology Consortium. The Gene Ontology resource: enriching a GOld mine. Nucleic Acids Res. 2021 Jan 8;49(D1):D325–34.

4. Ashburner M, Ball CA, Blake JA, Botstein D, Butler H, Cherry JM, et al. Gene Ontology: tool for the unification of biology. Nat Genet. 2000 May;25(1):25–9.

5. Wang Z, Gerstein M, Snyder M. RNA-Seq: a revolutionary tool for transcriptomics. Nat Rev Genet. 2009 Jan;10(1):57–63.

6. Hrdlickova R, Toloue M, Tian B. RNA-Seq methods for transcriptome analysis. Wiley Interdiscip Rev RNA. 2017;8(1).

7. Kukurba KR, Montgomery SB. RNA sequencing and analysis. Cold Spring Harb Protoc. 2015 Apr 13;2015(11):951–69.

8. Vandamme TF. Use of rodents as models of human diseases. J Pharm Bioallied Sci. 2014 Jan;6(1):2–9.

9. Sun X, Zhang W. Silencing of Gal-7 inhibits TGF-β1-induced apoptosis of human airway epithelial cells through JNK signaling pathway. Exp Cell Res. 2019 Feb 15;375(2):100–5.

10. Xu C, Yan T, Yang J. OVOL1 inhibits oral squamous cell carcinoma growth and metastasis by suppressing zinc finger E-box binding homeobox 1. Int J Clin Exp Pathol. 2019 Jul 1;12(7):2801–8.

11. Min H-Y, Sung YK, Kim E-J, Jang W-G. OVO homologue-like 1 promotes osteoblast differentiation through BMP2 expression. J Cell Physiol. 2019;234(7):11842–9.

12. Wang Y, Foo LY, Guo K, Gan BQ, Zeng Q, Hong W, et al. Syntaxin 9 is enriched in skin hair follicle epithelium and interacts with the epidermal growth factor receptor. Traffic. 2006 Feb;7(2):216–26.

13. Ampah KK, Greaves J, Shun-Shion AS, Asnawi AW, Lidster JA, Chamberlain LH, et al. S-acylation regulates the trafficking and stability of the unconventional Q-SNARE STX19. J Cell Sci. 2018 Oct 22;131(20).

14. Nair M, Bilanchone V, Ortt K, Sinha S, Dai X. Ovol1 represses its own transcription by competing with transcription activator c-Myb and by recruiting histone deacetylase activity. Nucleic Acids Res. 2007 Feb 20;35(5):1687–97.

15. Tsuji G, Ito T, Chiba T, Mitoma C, Nakahara T, Uchi H, et al. The role of the OVOL1-OVOL2 axis in normal and diseased human skin. J Dermatol Sci. 2018 Jun;90(3):227–31.

16. Kagawa H, Shimamoto R, Kim S-I, Oceguera-Yanez F, Yamamoto T, Schroeder T, et al. OVOL1 Influences the Determination and Expansion of iPSC Reprogramming Intermediates. Stem Cell Reports. 2019 Feb 12;12(2):319–32.

17. Li B, Nair M, Mackay DR, Bilanchone V, Hu M, Fallahi M, et al. Ovol1 regulates meiotic pachytene progression during spermatogenesis by repressing Id2 expression. Development. 2005 Mar;132(6):1463–73.

18. Nio-Kobayashi J. Tissue- and cell-specific localization of galectins, β-galactose-binding animal lectins, and their potential functions in health and disease. Anat Sci Int. 2017 Jan;92(1):25–36.

19. Barondes SH, Cooper DN, Gitt MA, Leffler H. Galectins. Structure and function of a large family of animal lectins. J Biol Chem. 1994 Aug 19;269(33):20807–10.

20. Chen Y-S, Chang C-W, Tsay Y-G, Huang L-Y, Wu Y-C, Cheng L-H, et al. HSP40 co-chaperone protein Tid1 suppresses metastasis of head and neck cancer by inhibiting Galectin-7-TCF3-MMP9 axis signaling. Theranostics. 2018 Jun 13;8(14):3841–55.

21. Trebo A, Ditsch N, Kuhn C, Heidegger HH, Zeder-Goess C, Kolben T, et al. High Galectin-7 and Low Galectin-8 Expression and the Combination of both are Negative Prognosticators for Breast Cancer Patients. Cancers (Basel). 2020 Apr 12;12(4).

22. Wang J, Liu Y, Yang Y, Xu Z, Zhang G, Liu Z, et al. High expression of galectin-7 is associated with poor overall survival in patients with non-metastatic clear-cell renal cell carcinoma. Oncotarget. 2016 Jul 5;7(27):41986–95.

23. Vetere A, Li WC, Paroni F, Juhl K, Guo L, Nishimura W, et al. OVO homologue-like 1 (Ovol1) transcription factor: a novel target of neurogenin-3 in rodent pancreas. Diabetologia. 2010 Jan;53(1):115–22.

24. Schulz H, Schmoeckel E, Kuhn C, Hofmann S, Mayr D, Mahner S, et al. Galectins-1, -3, and -7 Are Prognostic Markers for Survival of Ovarian Cancer Patients. Int J Mol Sci. 2017 Jun 8;18(6).

25. Babb RC, Chandrasekaran D, Zaugg LK, Sharpe PT. A mouse model to study reparative dentinogenesis. Methods Mol Biol. 2019;1922:111–9.

26. Whole genome - Mus_musculus - Ensembl genome browser 103 [Internet]. [cited 2021 Feb 16]. Available from: http://uswest.ensembl.org/Mus_musculus/Location/Genome

27. Feller L, Khammissa RAG, Schechter I, Thomadakis G, Fourie J, Lemmer J. Biological Events in Periodontal Ligament and Alveolar Bone Associated with Application of Orthodontic Forces. ScientificWorldJournal. 2015 Sep 2;2015:876509.

28. Holland R, Bain C, Utreja A. Osteoblast differentiation during orthodontic tooth movement. Orthod Craniofac Res. 2019 Aug;22(3):177–82.

29. Jiang N, Guo W, Chen M, Zheng Y, Zhou J, Kim SG, et al. Periodontal ligament and alveolar bone in health and adaptation: tooth movement. Front Oral Biol. 2016;18:1–8.

30. Joshi N, Hamdan AM, Fakhouri WD. Skeletal malocclusion: a developmental disorder with a life-long morbidity. J Clin Med Res. 2014 Dec;6(6):399–408.

31. Jaws: The Story of a Hidden Epidemic | Sandra Kahn and Paul R. Ehrlich [Internet]. [cited 2021 Feb 8]. Available from: https://www.sup.org/books/title/?id=29626

32. Kahn S, Ehrlich P, Feldman M, Sapolsky R, Wong S. The jaw epidemic: recognition, origins, cures, and prevention. Bioscience. 2020 Jul 22;

33. Singh VP, Sharma A. Epidemiology of malocclusion and assessment of orthodontic treatment need for nepalese children. Int Sch Res Notices. 2014 Dec 21;2014:768357.

34. Weinberger BW. Historical Résumé of the Evolution and Growth of Orthodontia**Read at the Seventy-Fifth Annual Session of the American Dental Association in conjunction with the Chicago Centennial Dental Congress, Aug. 7, 1933. The Journal of the American Dental Association (1922). 1934 Nov;21(11):2001–21.

35. Wahl N. Orthodontics in 3 millennia. Chapter 1: Antiquity to the mid-19th century. Am J Orthod Dentofacial Orthop. 2005 Feb;127(2):255–9.

36.Wahl N. The AJO-DO and the history of orthodontics. Am J Orthod Dentofacial Orthop. 2015 Nov;148(5):703–5.

37. Goyal S. The history of orthodontics. Am J Orthod Dentofacial Orthop. 2006 Dec;130(6):696–7.

38. How to spot and manage malocclusion in research mice [Internet]. [cited 2021 Jan 18]. Available from: https://www.jax.org/news-and-insights/jax-blog/2016/july/how-to-spot-malocclusion-in-research-mice

39. Balic A. Isolation of Dental Stem Cell-Enriched Populations from Continuously Growing Mouse Incisors. Methods Mol Biol. 2019;1922:29–37.

40. Sharir A, Marangoni P, Zilionis R, Wan M, Wald T, Hu JK, et al. A large pool of actively cycling progenitors orchestrates self-renewal and injury repair of an ectodermal appendage. Nat Cell Biol. 2019 Sep 2;21(9):1102–12.

41. Labrie M, Vladoiu M, Leclerc BG, Grosset A-A, Gaboury L, Stagg J, et al. A Mutation in the Carbohydrate Recognition Domain Drives a Phenotypic Switch in the Role of Galectin-7 in Prostate Cancer. PLoS ONE. 2015 Jul 13;10(7):e0131307.

42. Niiyama S, Yoshino T, Yasuda C, et al. Galectin-7 in the stratum corneum: a biomarker of the skin barrier function. *Int J Cosmet Sci*. 2016;38(5):487-495. doi:10.1111/ics.12326

Figure Legends

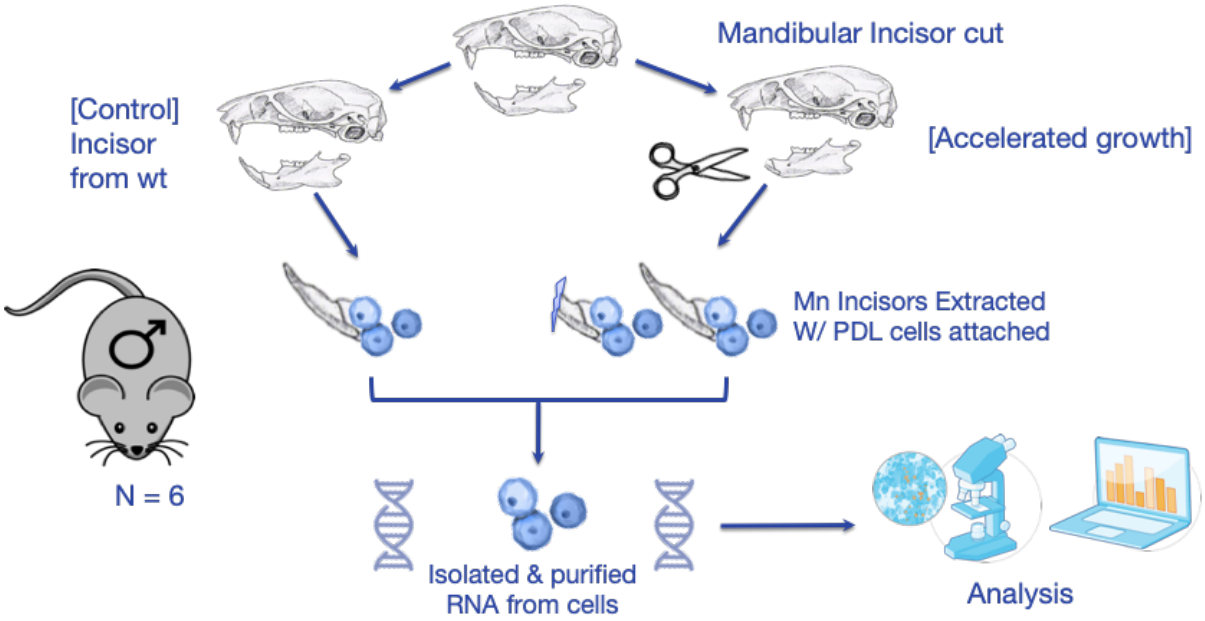

Figure 1. Workflow Diagram
Diagram showing overall project workflow. FVB/NJ mice were split into groups of three. Three of which had one incisor cut, the remaining were left alone. After 24 hours 3 groups of samples were collected. Those being an intact incisor from the control mice via extraction, the cut incisor from the experimental mice and the contralateral non-cut incisor from the experimental mice. These samples then underwent RNA isolation, purification, and analysis.

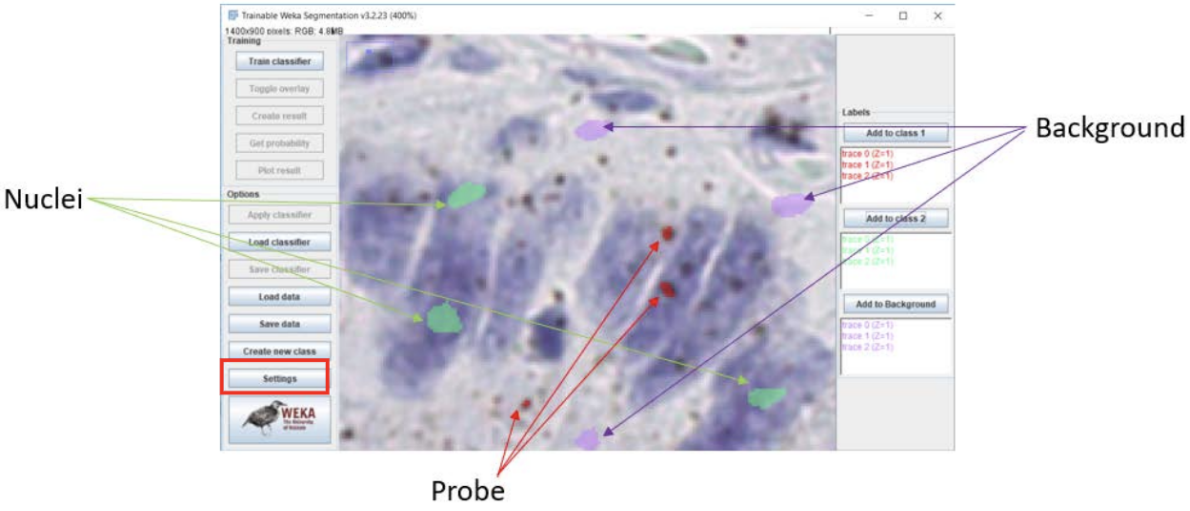

Figure 2. Reference view of software interface
ImageJ analysis software: digital interface, staining probes/cells and analysis tools.

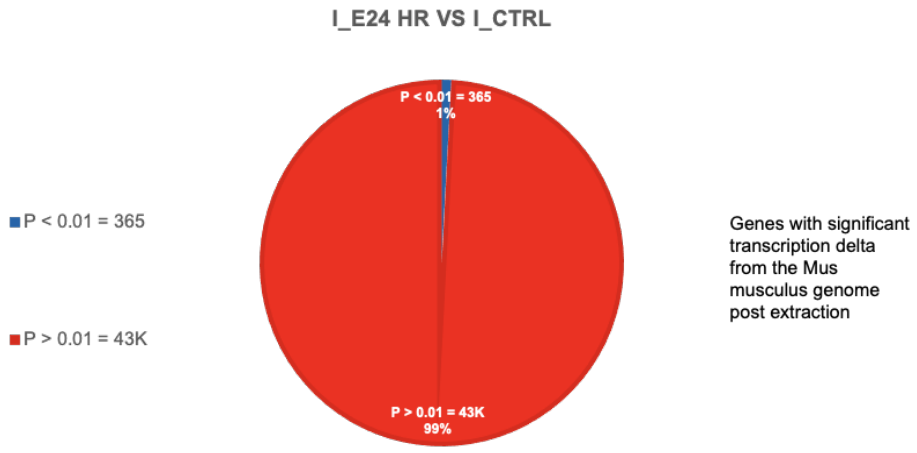

Figure 3. I_E24HR vs I_CTRL
Chart showing genes eliminated with application of a significant transcription delta (P<0.01) when comparing cut experimental incisors versus non-cut incisors from the control (wildtype) mice.

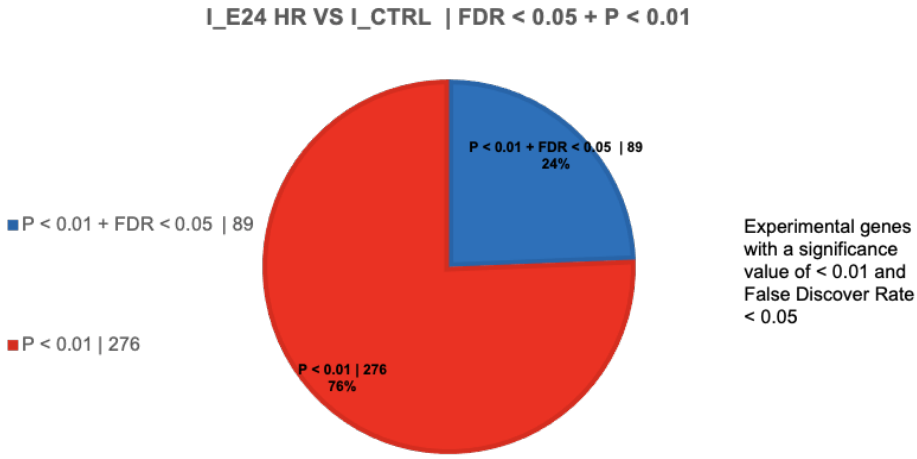

Figure 4. I_E24HR vs I_CTRL | FDR < 0.05 + P < 0.01
Chart showing genes eliminated with application of a significant transcription delta (P<0.01) and False Discovery Rate of < 0.05 when comparing cut experimental incisors versus non-cut incisors from the control (wildtype) mice.

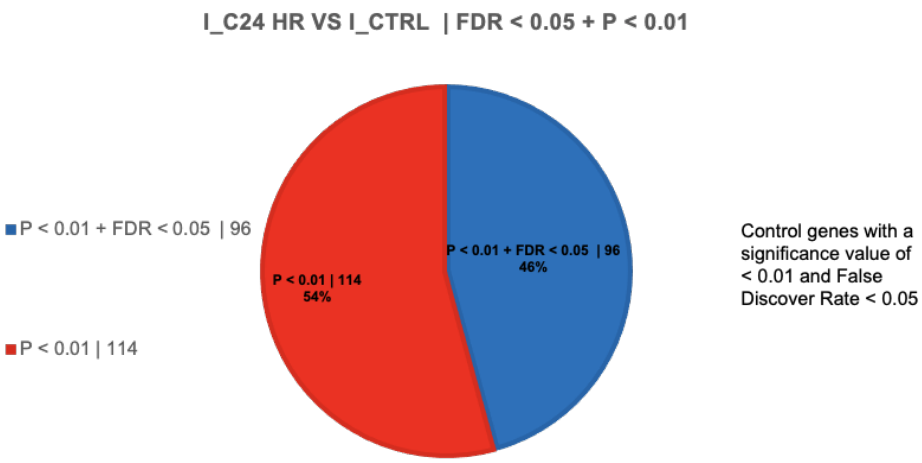

Figure 5. I_C24HR vs I_CTRL | FDR < 0.05 + P < 0.01
Chart showing genes eliminated with application of a significant transcription delta (P<0.01) and False Discovery Rate of < 0.05 when comparing non-cut contralateral incisors from the experimental mice versus non-cut incisors from the control (wildtype) mice.

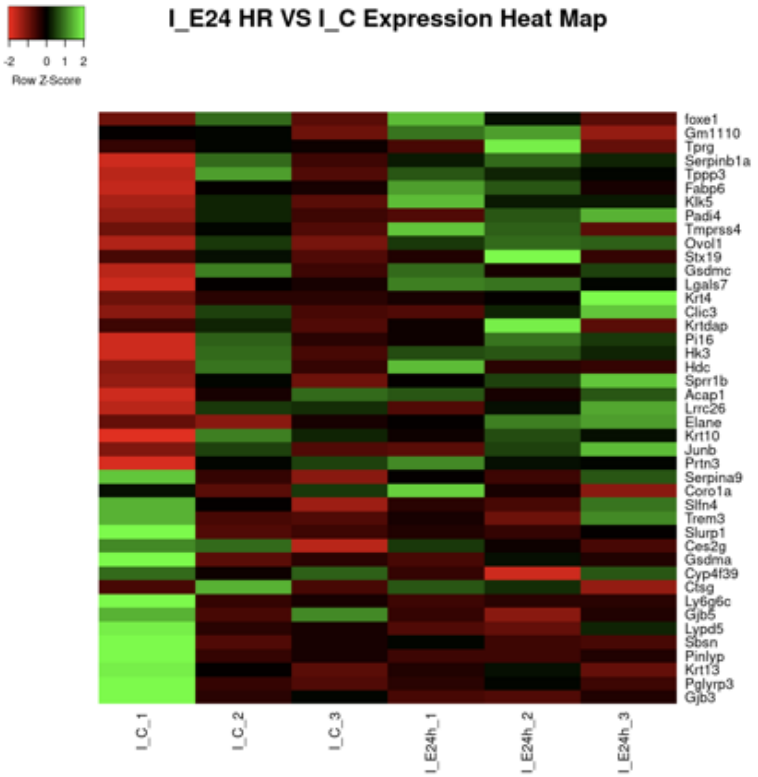

Figure 6. IE24 HR vs I_C Expression Heat Map
Heat map for visualization of gene expression levels with significant transcription deltas. A general increase or decrease in different genes can be appreciated when comparing the left 3 columns (control) versus the right three (experimental) .

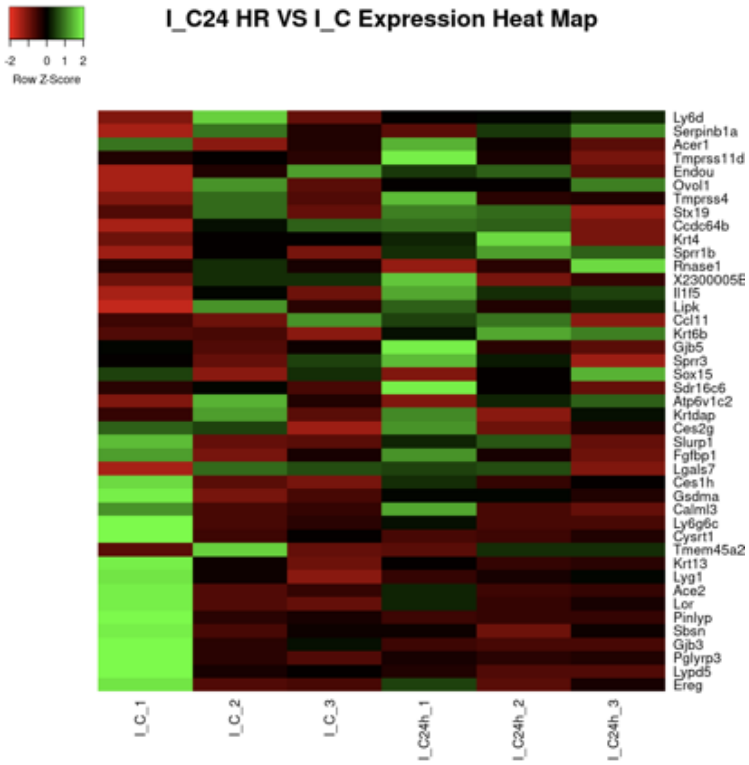

Figure 7. IC24 HR vs I_C Expression Heat Map
An RNA Heat map for visualizing expression levels, containing genes with significant transcription deltas. A general increase or decrease in different genes can be appreciated when comparing the left 3 columns (control) versus the right three (experimental) .

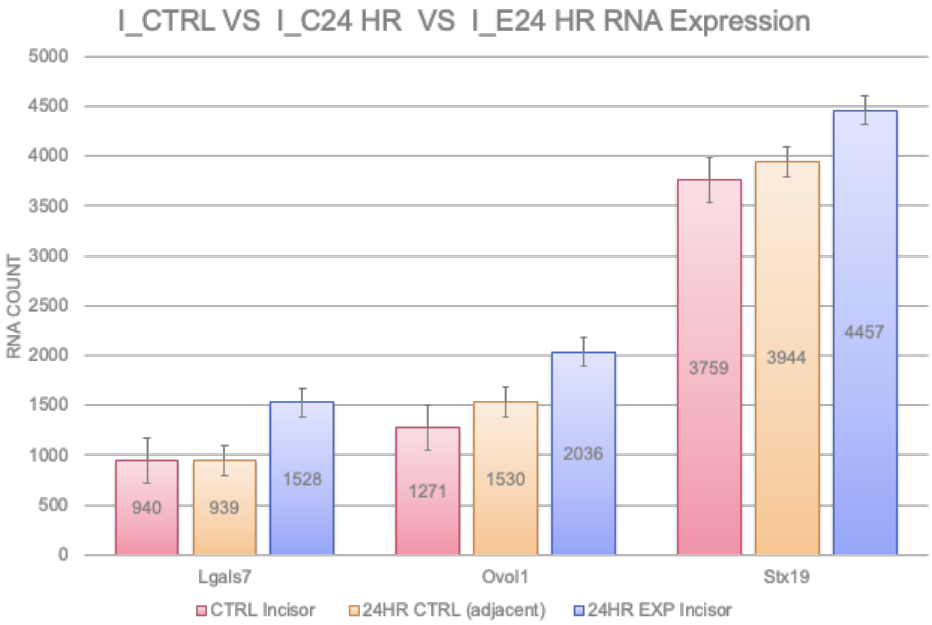

Figure 8. RNA expression
Expression levels of Lgals7, Ovol1, Stx19 at 24 hours for control, contralateral non cut and experimental cut incisor. Visualization of the upregulation of these three genes from our RNAseq values, Control incisor in red, adjacent non cut in yellow, and the experimental cut incisor in blue. We can see a mild increase in the adjacent non-cut incisor, and a larger increase in the experimental cut incisor.

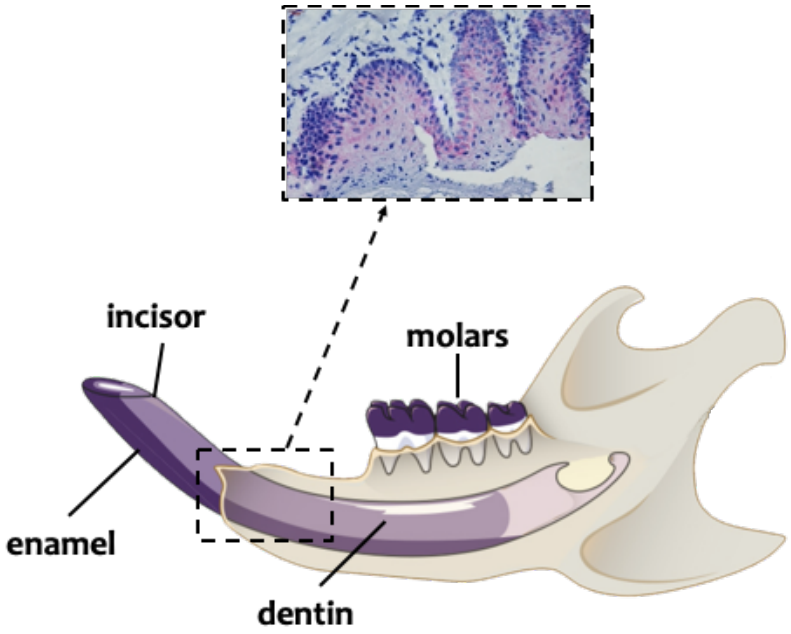

Figure 9. Region of interest
Region of interest on the lingual side of the cut incisors for RNAScope analysis. PDL-like tissues as well as gingival tissues attached immediately to the incisor base.

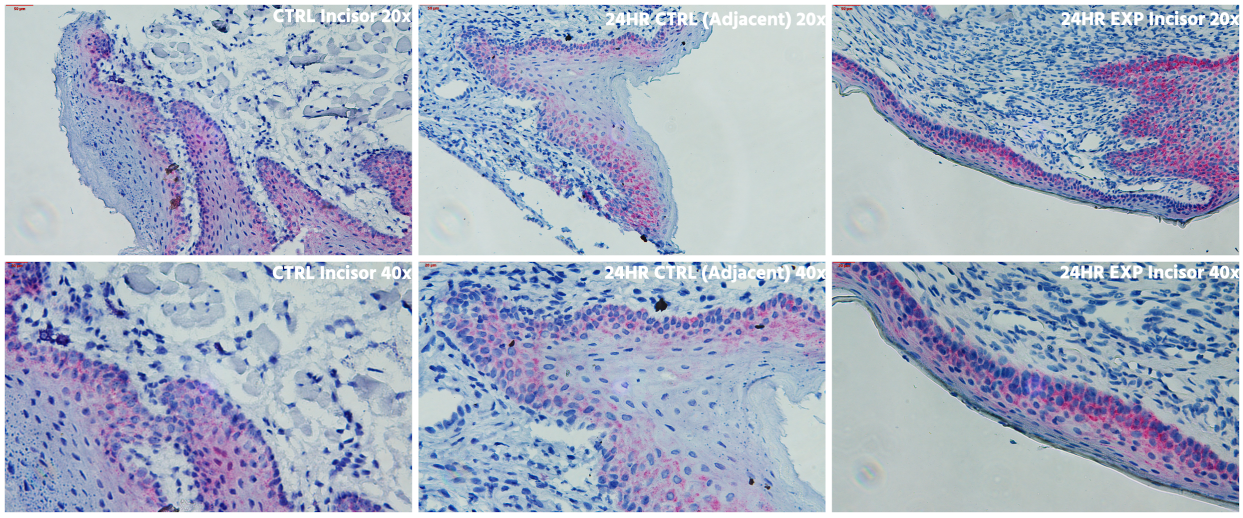

Figure 10. *Lgals7* RNAScope
Lgals7 expression (punctate dots) in gingival tissue at 20x and 40x magnification. The top and bottom are the same samples. A 50 micrometer red line in the top left corner demonstrates overall scale. Control incisors (CTRL) are in the first column, (adjacent incisor) in the second, and the experimental incisors (EXP) in the final column. A generalized marked increase in staining can be seen from left to right for *Lgals7* demonstrating increased expression. Expression is more concentrated in the basal epithelium, as well as the stratified epithelium.

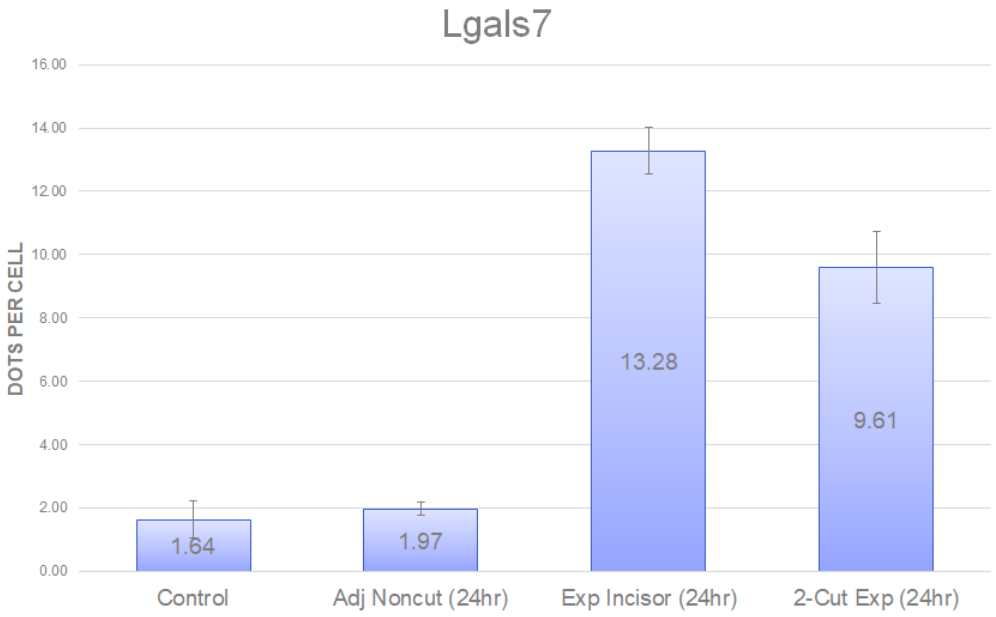

Figure 11. Expression levels of *Lgals7*
Quantification for *Lgals7* shows values for the control (wildtype) and adjacent incisors at 1.64 and 1.97 dots per cell, and increased expression at 13.28 and 9.6 dots per cell for the cut incisor groups confirming the increased expression of *Lgals7* during accelerated renewal.

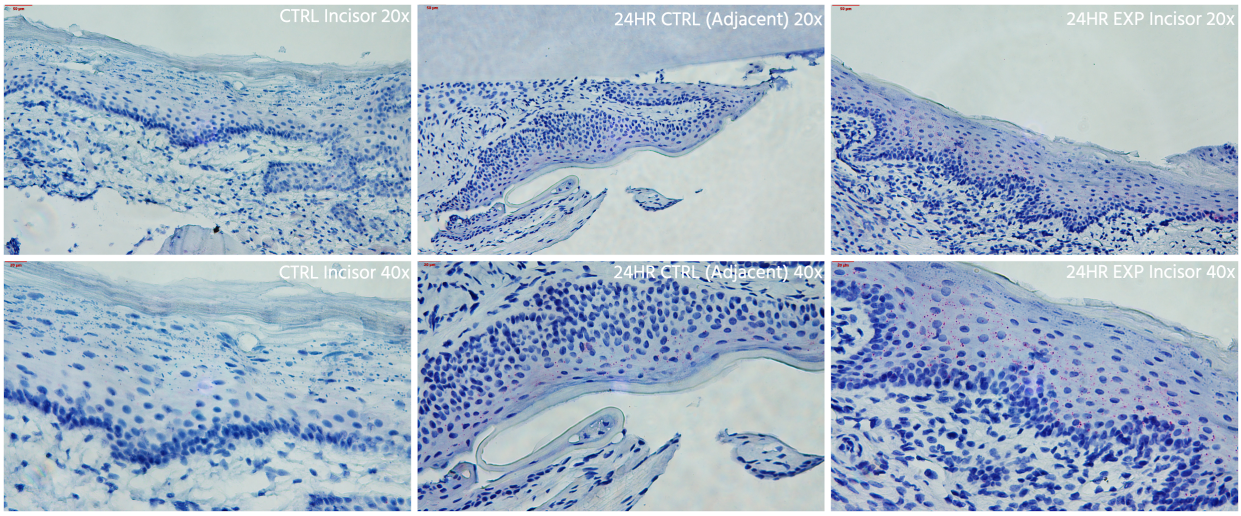

Figure 12. *Stx19* RNAScope

Stx19 expression (punctate dots) in gingival tissue at 20x and 40x magnification. The top and bottom are the same samples. A 50 micrometer red line in the top left corner demonstrates overall scale. Control incisors (CTRL) are in the first column, (adjacent incisor) in the second, and the Experimental incisors (EXP) in the final column. A generalized marked increase in staining can be seen from left to right for *Stx19* demonstrating increased expression. Expression is more concentrated in stratified epithelial cells but not in the basal epithelium or endothelium.

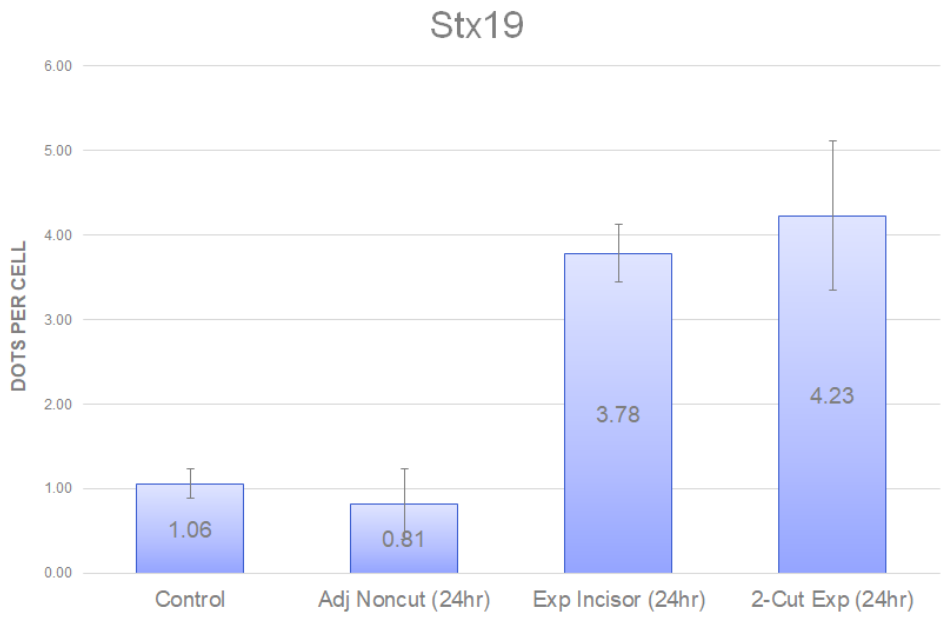

Figure 13. Expression levels of *Stx19*

Quantification for *Stx19* shows values for the control and adjacent incisors at 1.06 and 0.81 dots per cell, and increased expression at 3.78 and 4.23 dots per cell for the cut incisor group confirming increased *Stx19* expression during accelerated renewal.

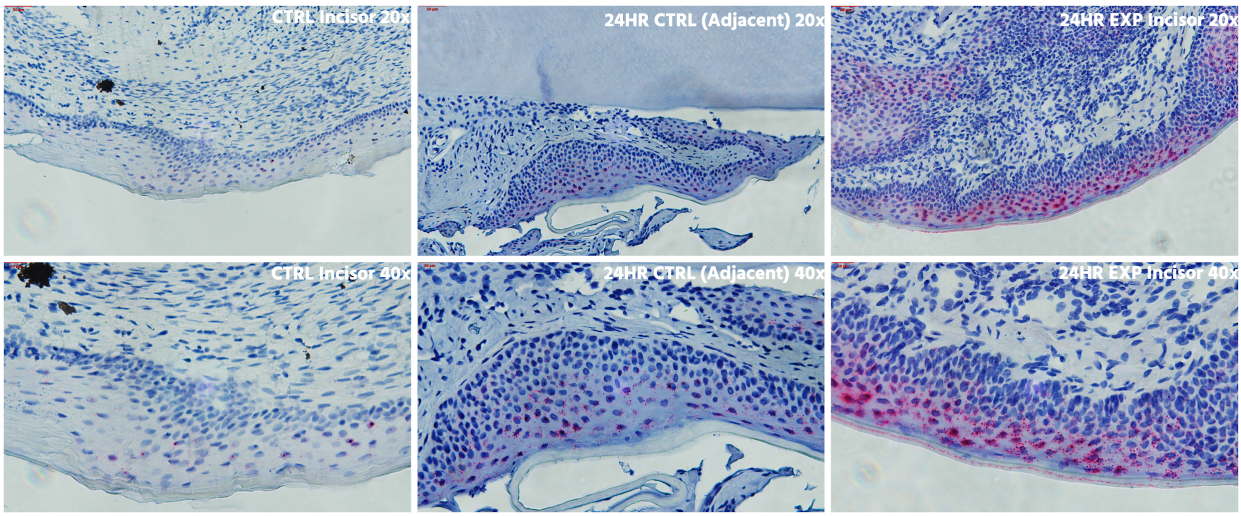

Figure 14. *Ovo1* RNAScope

Ovol1 expression (punctate dots) in gingival tissue at 20x and 40x magnification. The top and bottom are the same samples. A 50 micrometer red line in the top left corner demonstrates overall scale. Control incisors (CTRL) are in the first column, (adjacent incisor) in the second, and the Experimental incisors (EXP) in the final column. A generalized marked increase in staining can be seen from left to right for *Ovol1* demonstrating increased expression. Expression is in the stratified layer primarily but also present to a lesser degree in the keratinized layers as well.

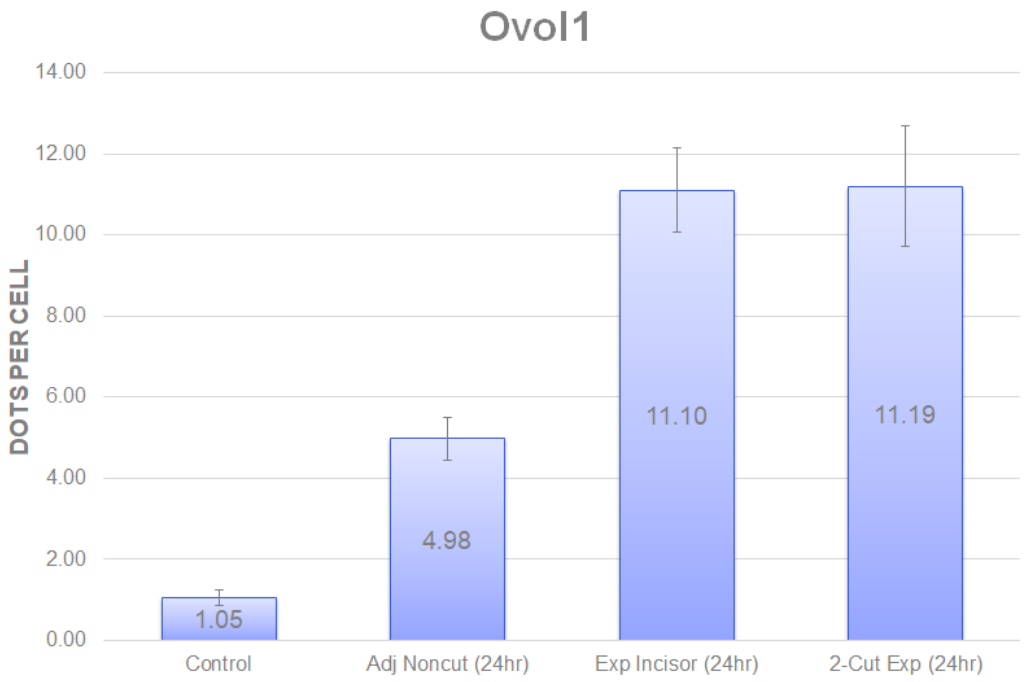

Figure 15. Expression levels of *Ovol1*

Quantification for *Ovol1* shows values for the control and adjacent incisors at 1.05 and 4.98 dots per cell, and increased expression at 11.10 and 11.19 dots per cell for the cut incisor group confirming the increased expression of the *Ovol1* during accelerated renewal.

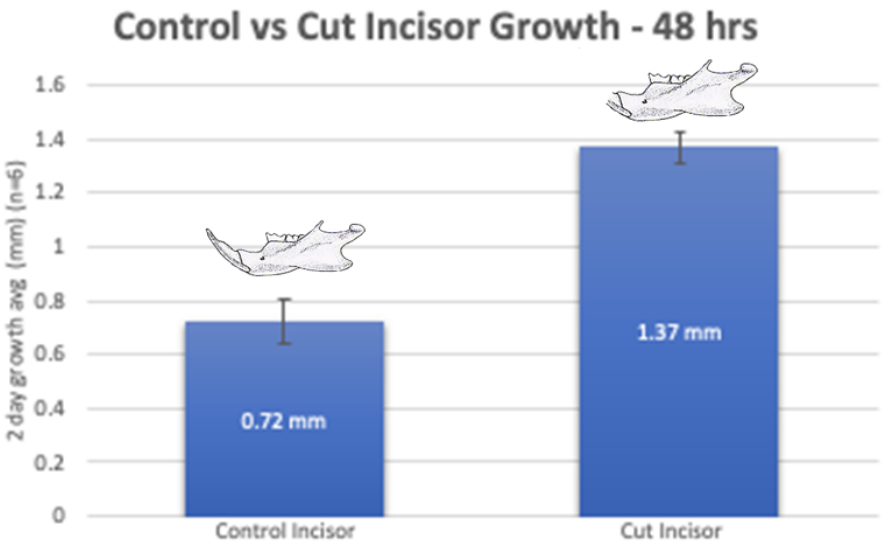

Figure 16. Control vs. Cut Incisor Growth - 48 hrs
To confirm that mouse incisors do indeed grow faster when out of occlusion, measurements were made on 6 mice, measuring 12 incisors total, half of which were cut and allowed to grow for two days. An average of 1.37 mm of growth was measured for the cut incisors and 0.72 mm for the uncut control incisors after the 48-hour period. Thus, FVB/NJ mouse incisors grow on average 0.68 mm per day when cut, and 0.36 mm in normal conditions.

Table 1. Background Research Example
Example information that was collected on all of the genes with the largest transcription deltas. Final genes of interest were thoroughly vetted as described in the results section.

Gene	Background Information
alox12b	This gene encodes an enzyme involved in the conversion of arachidonic acid to 12R-hydroxyeicosatetraenoic acid. Mutations in this gene are associated with nonbullous congenital ichthyosiform erythroderma.
krt4	This type II cytokeratin is specifically expressed in differentiated layers of the mucosal and esophageal epithelia with family member KRT13. Mutations in these genes have been associated with White Sponge Nevus, characterized by oral, esophageal, and anal leukoplakia
sprr1b	The protein encoded by this gene is an envelope protein of keratinocytes. The encoded protein is crosslinked to membrane proteins by transglutaminase, forming an insoluble layer under the plasma membrane
gsdmc	GSDMC (Gasdermin C) is a Protein Coding gene.The N-terminal moiety promotes pyroptosis
gsdma	GSDMA (Gasdermin A) is a Protein Coding gene. Diseases associated with GSDMA include Inflammatory Bowel Disease 22 and Gastric Cancer.
gjb3	This gene is a member of the connexin gene family. The encoded protein is a component of gap junctions
capns2	Calcium-regulated non-lysosomal thiol-protease which catalyzes limited proteolysis of substrates involved in cytoskeletal remodeling and signal transduction
stx19	Plays a role in endosomal trafficking of the epidermal growth factor receptor (EGFR). [injections of EGF cause premature eruption of teeth]
ly6d	May act as a specification marker at earliest stage specification of lymphocytes between B- and T-cell development. Marks the earliest stage of B-cell specification
serpinb1a	Neutrophil serine protease inhibitor that plays an essential role in the regulation of the innate immune response, inflammation and cellular homeostasis
endou	This gene encodes a protein with protease activity and is expressed in the placenta. The protein may be useful as a tumor marker.
calml3	CALML3 (Calmodulin Like 3) is a Protein Coding gene. Diseases associated with CALML3 include Acanthoma and Alzheimer Disease. Among its related pathways are Oxytocin signaling pathway and Salivary secretion.
gjb5	The encoded protein is a gap junction protein involved in intercellular communication related to epidermal differentiation and environmental sensing.
tmprss4	This gene encodes a member of the serine protease family. Serine proteases are known to be involved in a variety of biological processes, whose malfunction often leads to human diseases and disorders.
acer1	Is a skin-specific ceramidase that regulates the levels of ceramides, sphingosine and sphingosine-1-phosphate in the epidermis, mediates the calcium-induced differentiation of epidermal keratinocytes and more generally plays an important role in skin homeostasis
ovol1	This gene encodes a putative zinc finger containing transcription factor that is highly similar to homologous protein in Drosophila and mouse. Based on known functions in these species, this protein is likely involved in hair formation and spermatogenesis in human as well. 13OVOL1 is required for osteoblast differentiation by inducing BMP2 expression in MC3T3-E1 cells

Publishing Agreement

It is the policy of the University to encourage open access and broad distribution of all theses, dissertations, and manuscripts. The Graduate Division will facilitate the distribution of UCSF theses, dissertations, and manuscripts to the UCSF Library for open access and distribution. UCSF will make such theses, dissertations, and manuscripts accessible to the public and will take reasonable steps to preserve these works in perpetuity.

I hereby grant the non-exclusive, perpetual right to The Regents of the University of California to reproduce, publicly display, distribute, preserve, and publish copies of my thesis, dissertation, or manuscript in any form or media, now existing or later derived, including access online for teaching, research, and public service purposes.

DocuSigned by:
D471123E5F984C1...
Author Signature

5/23/2021
Date